

CSIS Discussion Paper No. 112

**Prospective Space-Time Analysis of the 2007 Cryptosporidiosis
Outbreak, Salt Lake County, Utah**

Marissa Taddie ^a and Ikuho Yamada ^b

June 2012

a) Ph.D. Student, Department of Geography, University of Utah, USA

b) Associate Professor, Interfaculty Initiative in Information Studies, and Center for
Spatial Information Science, University of Tokyo

Abstract

Cryptosporidiosis is a gastrointestinal illness caused by a protozoan parasite that is highly contagious and resistant to multiple disinfectants. Utah experienced a large, communitywide outbreak of cryptosporidiosis between June and December of 2007. Nearly forty percent of laboratory-confirmed cases occurred in Salt Lake County (SL County), Utah. Using this case data, our study investigated if prospectively applied space-time surveillance could have detected any significant clusters as cases were reported to Salt Lake Valley Health Department (SLVHD). This study utilized a space-time scan statistic to test for the occurrence and location(s) of cryptosporidiosis clusters using time-periodic prospective surveillance and a Poisson probability model. Report dates were used in the prospective space-time analysis to replicate the realistic surveillance processes that occur in health departments and to mimic a near real-time surveillance system. The first cluster signaled approximately 20 days after the first reported case in SL County. This cluster occurred two days before a statewide press release was issued and 21 days prior to the implementation of major intervention measures. From August through mid-September many significant clusters were detected throughout the county. The results of this study suggest that there were distinct spatio-temporal patterns throughout the outbreak period. Therefore, space-time analysis would have been a valuable and complementary tool to temporal surveillance since it could have detected spatial clusters and high-risk areas of disease as they were reported, or emerged. In addition, it may have been useful for targeting intervention strategies and prioritizing investigations during this large communitywide outbreak.

Introduction

Over the last thirty years, there has been a substantial rise in waterborne disease outbreaks (WBDOs) associated with both natural and treated recreational water across the United States (Yoder et al., 2008). Of the 48 gastroenteritis WBDOs that occurred between 2005 and 2006, *Cryptosporidium* spp. was implicated in 31 of the outbreaks (Yoder et al., 2008). These “crypto” outbreaks caused thousands of illnesses, and the majority of these were associated with treated (chlorinated) recreational water (Yoder et al., 2008). Since *Cryptosporidium* and its oocysts are immediately infective and resistant to common treatments used in recreational waters, early detection of *Cryptosporidium* outbreaks is needed to quickly identify at-risk areas and implement intervention measures.

During the summer and fall months of 2007, Utah experienced its first large, communitywide outbreak of cryptosporidiosis (UDOH, 2008; SLVHD, 2008). In past years, the state average was approximately 14.8 cases per year and SL County, which is located at the center of the state and accounted for about 38% of the state population in 2007 (U.S. Census Bureau, 2007), averaged fewer than five cases annually (UDOH, 2008; SLVHD, 2008). From June through December of 2007, the Utah Department of Health (UDOH) received reports of 1,902 laboratory-confirmed cryptosporidiosis cases across the state (UDOH, 2008). Approximately 38% of the laboratory-confirmed cases (718 cases) occurred in SL County and the incidence rate for the entire outbreak in the county was 125.9 per 100,000 person-years (UDOH, 2008). In SL County, the bulk of cases were reported between July 19 and December 5, 2007 (UDOH, 2008; SLVHD, 2008). Swimming in recreational water was considered a significant risk factor during

the summer months and ongoing person-to-person transmission may have protracted the outbreak into the fall (UDOH, 2008; SLVHD, 2008).

Health departments rely on a number of active, passive, and syndromic surveillance methods to detect outbreaks in the community. Many times, reported cases of disease are the first clue of an emerging outbreak and trigger subsequent case investigations. Ongoing temporal surveillance is used to establish (or examine) trend lines, risk factors, and the changing dynamics of an outbreak as more information is gathered. The spatial component of an outbreak is generally not an explicit part of the time series analysis, however being able to identify geographic clusters as cases are reported to the health department may help elucidate areas of elevated risk, prioritize case investigations, and customize or target interventions strategies.

Using SL County's 2007 cryptosporidiosis case data, this study investigated if prospectively applied space-time surveillance could have detected any significant, emerging clusters as cases were reported to SLVHD. To achieve this objective, this study utilized a space-time scan statistic to analyze case-specific data. While true disease outbreaks should be characterized by the onset date of each case, health departments' surveillance systems often rely upon the date the case is reported since this is the first piece of case-specific information available to the departments and onset dates are not collected until after an investigation is started. Therefore, this study utilized report dates in the prospective space-time analysis to replicate the realistic surveillance processes that occur in health departments and to mimic a near real-time surveillance system.

Background

Cryptosporidium occurs worldwide and is a protozoan parasite that causes gastrointestinal infections in both human and animals (Fayer & Xiao, 2008; APHA, 2004). Currently, there are at least 16 species as well as a number of different genotypes of *Cryptosporidium*; *C. hominis* and *C. parvum* are most commonly associated with human cryptosporidiosis (Fayer & Xiao, 2008; APHA, 2004). Cryptosporidiosis can occur in both immunocompetent and immunocompromised persons (Chen, Keithly, Paya, & LaRusso, 2002; Huang & White, 2006; APHA, 2004). Once a host is infected, the parasite generally becomes established in the small intestine, reproduces, and its infective oocysts are then shed in the stool (Fayer & Xiao, 2008; Chen et al., 2002; Huang & White, 2006; APHA, 2004).

Oocysts are immediately infective and are characterized by a thick outer wall (Fayer & Xiao, 2008; APHA, 2004). This wall serves as protection and allows the pathogen to survive outside of the body for long periods of time in moist conditions (Fayer & Xiao, 2008; APHA, 2004). Between 10^8 - 10^9 oocysts can be shed in a single bowel movement (Yoder & Beach, 2007). *Cryptosporidium* oocysts are resilient and have proven to be resistant to a number of aldehyde-, ammonia-, alcohol-, alkaline-, and chlorine-based cleaning products (Fayer & Xiao, 2008; Chen et al., 2002; Huang & White, 2006). Normal chlorination levels in recreational swimming pools do not inactivate the infective parasite ((Fayer & Xiao, 2008; Huang & White, 2006), and studies have demonstrated that even after exposure to household bleach for two hours, the oocyst is still infectious (Huang & White, 2006). Research suggests that oocysts are sensitive to hydrogen peroxide, ozone, and ultraviolet (UV) radiation (Huang & White, 2006).

Cryptosporidium transmission follows a fecal-oral route and infection occurs when a susceptible host ingests the infective oocysts (Fayer & Xiao, 2008; APHA, 2004). Transmission can be person-to-person, animal-to-person, or from any soil, food, water, or surface that has become contaminated with fecal matter (Fayer & Xiao, 2008; APHA, 2004). The infectious dose is low and between 10-30 oocysts can trigger an infection (Yoder & Beach, 2007). Symptoms generally appear one to two weeks after exposure, with seven being the average (APHA, 2004), and twenty-one days is generally considered the maximum incubation period (Fayer & Xiao, 2008). Infected persons may be asymptomatic or symptomatic. When symptoms are present they are dominated by watery diarrhea, stomach cramps, nausea, weight loss, low-grade fever, and vomiting (APHA, 2004). Symptoms can persist from two days to one month and fecal shedding of oocysts can continue up to 50 days after the last bout of diarrhea (Yoder & Beach, 2007).

Methods

Study area and data collection

The study area included Salt Lake County, Utah, which consisted of 567 census block groups (U.S. Census Bureau, 2000a). Data on 677 laboratory-confirmed cryptosporidiosis cases were acquired from the SLVHD and included all cryptosporidiosis cases reported between June 1, 2007 and November 1, 2007 in SL County. Case data contained information on age, gender, place of residence, zip code, date of disease onset, date reported to SLVHD, and laboratory date. Population data was obtained from the U.S. Census Bureau, using the July 1, 2006 population estimates (U.S. Census Bureau, 2006). The study area encompassed approximately 737 square miles

(1908.82 square kilometers (km)) and included a population of 978,701 individuals, which was approximately 38 percent of the state's population (U.S. Census Bureau, 2006). This project was approved by the University of Utah Institutional Review Board.

Data preprocessing

To prepare the data for analysis, case data was geocoded at the block group level. Of the 677 laboratory-confirmed cases, 670 cases (99%) were successfully geocoded. Secondary cases within households were then excluded (52 cases) to avoid unfairly weighting the statistic, which left 618 primary cases for the subsequent analysis. The block group population was calculated using July 1, 2006 county-level estimates by distributing it proportionally to the census 2000 population (U.S. Census Bureau, 2000b) at the block group level. The result of the data preprocessing was two sets of data at the same resolution: case counts and population counts for each block group in SL County.

Statistical methodology

A space-time scan statistic implemented in SaTScan software (Kulldorff & Information Management Services, 2007) was used to test for the occurrence and location(s) of cryptosporidiosis clusters using time-periodic prospective surveillance and a Poisson probability model (Kulldorff, 1997; Kulldorff & Information Management Services, 2007; Kulldorff, 2001; Kulldorff, Athas, Feurer, Miller, & Key, 1998; Kleinman, Abrams, Kulldorff, & Platt, 2005). The space-time scan statistic is based on both a spatial and temporal window (Kulldorff, 1997; Kulldorff, 2001). These windows vary from a minimum spatial distance and temporal length up to user-defined maximum distance and time. In searching for clusters, or high rates, the space-time scan statistic generates a large number of variably sized space-time cylinders that are located across

the study region (Kulldorff, 1997; Kulldorff, 2001; Kulldorff et al., 1998; Kleinman et al., 2005). Each space-time cylinder yields a likelihood ratio based on whether the observed number of cases within a cylinder is greater than would be expected if the cases were distributed randomly in space and time with respect to the underlying population (Kulldorff, 1997; Kulldorff, 2001; Kulldorff et al., 1998). The cylinder with the maximum likelihood ratio is reported as the most likely cluster (Kulldorff, 1997; Kulldorff, 2001; Kulldorff et al., 1998). Significance is assessed using Monte Carlo hypothesis testing (Dwass, 1957).

Case data provided by the SLVHD included onset date, laboratory date, and report date. Given that the goal of this analysis was to imitate a near real-time surveillance system and the report date was the first piece of case-specific information available to epidemiologists during the outbreak, a decision was made to use the report date in the space-time analysis. Report dates represent when SLVHD became aware of laboratory-confirmed cryptosporidiosis cases in their jurisdiction. Hence, clusters detected based on reports date would correspond to what SLVHD could have detected by incorporating the space-time prospective surveillance into their routine surveillance system during the summer and fall months of 2007.

The maximum spatial cluster size was a circle with a 2.5-mile (4.02 km) radius and the maximum temporal cluster size was seven days. The study period, or time step, for the analysis was 28 days, which was determined by using the maximum incubation period, generally considered to be 21-days, and then adding seven days to capture the person reported on day 21. The first reported cryptosporidiosis case occurred on July 19 and the last reported case included in this study was on October 22, so that daily analysis

in this study began 28 days prior to the first reported case and finished 28 days after the last reported case in October. Therefore, 151 separate daily analyses were conducted from June 22 to November 18. The 28-day study period stepped forward through time as one day was added and one day was removed during the outbreak. In order to imitate a prospective space-time analysis, cases that were outside of the time step were ignored.

Prospective surveillance necessitates a modification in the space-time scan statistic due to the multiple testing problem inherent in repeated time-periodic surveillance (Kulldorff, 2001). Therefore, an adjustment was made for earlier analysis, which resulted in a p -value that was corrected for the repeated surveillance (Kulldorff, 2001; Kulldorff, 2007; Kleinman et al. 2005). SaTScan provides both a p -value and a recurrence, or null occurrence, interval for prospective analysis (Kulldorff, 2007). The recurrence interval is how often one would expect to see the cluster just by chance if the null hypothesis is true (Kulldorff, 2001, 2007). In this study, 999 Monte Carlo replications were used to assess significance and thus the smallest p -value obtainable was 0.001. This significance level corresponded with a recurrence interval of once every 76.6 years when adjusted for earlier analyses within the 28-day study period. A recurrence interval of approximately 1 year, corresponding with a p -value of approximately 0.074, was used as the cut off to summarize the results.

Results

From June 22 to November 18, forty-seven clusters were detected. Table 1 contains only the space-time clusters that were representative of the patterns that emerged during the early, middle, and late stages of the outbreak. In this table a total of 14

clusters are listed and grouped into six 28-day time steps based on the first day of the signal. A complete table summarizing all signals is available by request from the authors. Figure 1 also summarizes all significant space-time clusters graphically and shows the general geographic region where the clusters emerged. It is important to note that one cluster can correspond to multiple signals. For example, the first cluster was detected on August 8 and continued to signal until August 12. The six 28-day time steps listed in the table are discussed below to illustrate the general pattern of cluster emergence that developed across SL County in the summer and fall months of 2007.

The first laboratory-confirmed cryptosporidiosis case was reported to SLVHD on July 19, 2007 (Morbidity and Mortality Weekly Report (MMWR) Week 29), and the first significant space-time signal (Figure 2a) was detected 21 days later on August 8, 2007 (MMWR Week 32). This cluster occurred two days before a statewide press release was issued by the UDOH warning people to avoid swimming while ill and 21 days prior to the implementation of major intervention measures. During this 28-day time step, there were 20 reported cases and 12 of them were reported during the last week of the time step (MMWR Week 32). The space-time signal ($p = 0.001$; recurrence interval = 76.6 yrs) included one block group and was triggered by three cases observed over two days when the expected number of cases was 0.01, which produced a relative risk of approximately 581.7 (Signal ID 1 in Table 1). This initial cluster remained persistent through time as subsequent daily analyses also showed this cluster as significant until August 12. As expected, the significance of the cluster decreased on each subsequent day of analysis since the space-time scan statistic adjusted for multiple testing.

Figure 2b shows a larger cluster ($p = 0.019$; recurrence interval = ~ 4 yrs) that was observed on the opposite side of the county on August 17. This cluster extended across 48 block groups and included 51 cases in the time step, of which 29 of them were reported during the week ending on August 18 (MMWR Week 33). The space-time cluster was triggered by eight cases observed over four days when the expected number of cases was 0.65, which produced a relative risk of approximately 14.4 (Signal ID 6 in Table 1).

Figure 2c shows two large space-time clusters were detected on opposite sides of the county on August 21. During this time step there were a total of 76 cases. The most likely cluster ($p = 0.006$; recurrence interval = 12.7 yrs) occurred on the west side of SL county, extended across 14 block groups, and had six cases observed over two days, which was approximately 32.8 times greater than expected (Signal ID 8 in Table 1). The secondary cluster ($p = 0.024$; recurrence interval = 3.1 yrs) was found on the east side of the county, included 53 block groups, and included 12 cases observed over seven days, which was approximately 7.7 times more cases than expected (Signal ID 8a in Table 1).

Figure 2d shows three significant space-time clusters across the county. During this time step there were a total of 127 cases. The most likely cluster ($p = 0.001$; recurrence interval = 76.6 yrs) on the west side of the county still contained the same block groups as seen on August 21, but the number of cases has increased from six to 11 observed over five days, which was approximately 14.4 times more cases than expected (Signal ID 11 in Table 1). The secondary cluster ($p = 0.048$; recurrence interval = 1.5 yrs) was also similar to the cluster observed on the east side of the county on August 21, but is spatially more compact, extending across 32 block groups. This cluster included

six cases observed over one day, which was 22.0 times greater than expected (Signal ID 11a in Table 1). The tertiary cluster ($p = 0.053$; recurrence interval = 1.4 yrs) was the northern most signal during this time step and included eight cases observed over two days across 54 block groups, which was 12.3 times more cases than expected (Signal ID 11b in Table 1).

On September 7, four significant clusters were detected across the county (Figure 2e). During this time step there were a total of 342 cases. The most likely cluster occurred on the west side of the county, extended across 23 block groups, and included 25 cases observed over four days, which was 9.5 times greater than expected (Signal ID 21 in Table 1). The secondary cluster occurred near the southern edge of the county, extended across 16 block groups, and included 19 cases observed over four days, which was 10.1 times more cases than expected (Signal ID 21a in Table 1). The tertiary cluster was the northern most signal, extended across 25 block groups, and included 15 cases observed over four days, which was 9.8 times greater than expected (Signal ID 21b in Table 1). The p -value for all three of these clusters was 0.001, which corresponded to a recurrence interval of 76.6 years. The fourth signal ($p = 0.011$; recurrence interval = 6.9 yrs) included 16 block groups and occurred between the most likely and secondary clusters, which could indicate spatial diffusion between the two areas. This cluster included 13 cases observed over four days, which was 7.2 times greater than expected (Signal ID 21c in Table 1).

The last signals were detected on September 11, when the epidemic had begun declining (Figure 2f). During this time step there were a total of 401 cases. The most likely cluster ($p = 0.001$; recurrence interval = 76.6 yrs) on the west side of the county

still contained the same block groups as seen on September 7, but the number of cases has increased from 19 to 25 observed over seven days, which was approximately 4.5 times more cases than expected (Signal ID 25 in Table 1). The secondary cluster ($p = 0.003$; recurrence interval = 25.5 yrs) was again near the southern edge of the county, extended across six block groups, and included 15 cases observed over seven days, which was 7.1 times more cases than expected (Signal ID 25a in Table 1). The final cluster ($p = 0.021$; recurrence interval = 3.6 yrs) was again located between the most likely and secondary clusters, extended across 12 block groups, and included 15 cases observed over seven days, which was 5.9 greater than expected (Signal ID 25b in Table 1).

Discussion and Conclusions

This study demonstrated that by utilizing a time-periodic prospective surveillance system, it may have been possible to detect high-risk areas of the outbreak that were emerging from the cases being reported on a daily basis. While report dates clearly lag behind onset dates, this is a limitation faced by health departments within the framework of the National Notifiable Disease Surveillance System (NNDSS) (Buehler et al., 2004). Within the constraints of this system, health departments only become aware of specific cases of reportable diseases when they are notified by health care providers and/or laboratories. While a variety of syndromic surveillance systems (e.g., chief complaint logs, quantity of over-the-counter pharmaceuticals, school absenteeism, etc) can signal the initiation of an outbreak in its early stages, determining the risk or causal factors associated with the outbreak depends largely on timely and thorough case investigations of reported disease cases.

Report dates represent when SLVHD became aware of specific instances of cryptosporidiosis cases within their jurisdiction. This outbreak quickly overwhelmed the resources of the SLVHD and as noted by SLVHD, "...[the] outbreak was incredibly resource intensive and demanded that priorities be shifted, all [the while] maintaining regular disease surveillance and investigation" (SLVHD, 2008, pg. 5). While it was clear that cases were being reported from throughout the county, temporal surveillance methods did not enable the investigators to discern if areas of excess risk were emerging from the large number of daily reports. For instance, five of the six time steps presented above clearly illustrate that the signal located on the west side of the county perpetuated throughout the entire period clusters were detected and only grew to include more cases throughout August and September. Knowing this information might have helped local officials prioritize the investigations and target interventions during this communitywide outbreak.

Underreporting and time lags certainly affected the detection of the outbreak in its early stages. However, previous research suggested that even with time lags of two weeks, prompt and efficient action can limit the transmission potential (Yoder et al., 2008). Quickly identifying areas of elevated risk in conjunction with case investigations may help elucidate common sets of risk factors or generate hypotheses as to the source(s) of the outbreak. As noted earlier, swimming in recreational water was considered a significant risk factor in becoming ill with cryptosporidiosis. Therefore, by visually mapping the locations of significant space-time clusters in conjunction with risk factors obtained through investigational notes, it may have been possible to determine if various recreational water venues, or other risk factors, were being implicated by the significant

clusters. This type of visualization effort might have allowed more targeted intervening efforts at the beginning of the outbreak.

In a smaller outbreak with fewer daily reports, it would be easier to investigate and map potential exposure sources of *all* reported cases. However, with the large number of cases that were reported on a daily basis during this outbreak, mapping individual exposure sources in a timely manner would have not only become difficult, but it would have been hard to visualize and tease apart any potential commonalities or unique spatial patterns. By utilizing a time-periodic prospective surveillance system, it was possible to detect space-time clusters that were emerging from the daily case reports. Through the integration of space-time analysis, temporal surveillance, and risk factor mapping it may have also been possible to evaluate if there were commonalities in potential exposure sources and determine if the exposures were changing based on the detection of different or expanding clusters.

The results are subject to various limitations due to the manner in which the data was reported, geocoded, and analyzed. First, addresses were self-reported by cases and there may have been bias in the reported address as well as the geocoding of those addresses. Second, report date heaping by the various labs may have resulted in less temporal variability, which can impact the results of the analysis. Third, underreporting and lag times between onset and report dates certainly affected the detection of the outbreak in its early stages. Furthermore, it is possible that people with the earliest onset may not have been the first to be reported. Fourth, there may be uncertainties associated with the cluster boundaries due to two specific limitations. First, given that case data was geocoded at the block group level, significant space-time clusters represent combinations

of contiguous block, which may or may not correspond to the true boundaries of high-risk areas. Second, the maximum spatial cluster size parameter, which was set to a circle with a 2.5-mile (4.02 km) radius, may have restricted the size of the maximum cluster detected. Future sensitivity analysis could help assess the potential impact of this parameter setting.

Additional information provided by prospectively applied space-time surveillance could be useful to local officials needing to quickly identify at-risk areas, implement intervention or quarantine measures, and control or limit public exposure. This seems especially relevant to large outbreaks that are associated with multiple exposure sources. The results of this study suggest that there were distinct spatio-temporal patterns throughout the outbreak period. Therefore, space-time analysis would have been a valuable and complementary tool to temporal surveillance since it could have detected spatial clusters and high-risk areas of disease as they were reported, or emerged. In addition, it may have been useful for targeting intervention strategies and prioritizing investigations during this large communitywide outbreak.

References

- American Public Health Association. (2004). Cryptosporidiosis. In D. L. Heymann (Ed.), *Control of Communicable Diseases Manual* pp. 138-141). Washington, DC: American Public Health Association.
- Buehler, J. W., Hopkins, R. S., Overhage, J. M., Sosin, D. M., & Tong, V. (2004). Framework for evaluating public health surveillance systems for early detection of outbreaks. *MMWR Surveillance Summaries*, 53(RR05), 1-11.
- Chen, X.-M., Keithly, J. S., Paya, C. V., & LaRusso, N. F. (2002). Cryptosporidiosis. *New England Journal of Medicine*, 346(22), 1723-1731.
- Dwass, M. (1957). Modified randomization tests for non-parametric hypothesis. *Annals of Mathematical Statistics*, 28, 181-187.
- Fayer, R., & Xiao, L. (Eds.) (2008). *Cryptosporidium and Cryptosporidiosis*. Boca Raton, FL: Taylor and Francis Group, LLC.
- Huang, D. B., & White, A. C. (2006). An updated review on *Cryptosporidium* and *Giardia*. *Gastroenterology Clinics of North America*, 35, 291-314.
- Kleinman, K. P., Abrams, A. M., Kulldorff, M., & Platt, R. (2005). A model-adjusted space-time statistic with an application to syndromic surveillance. *Epidemiology and Infections*, 133, 409-419.
- Kulldorff, M. (1997). A spatial scan statistic. *Communications in Statistics: Theory and Methods*, 26(6), 1481-1496.
- Kulldorff, M. (2001). Prospective time periodic geographical disease surveillance using a scan statistic. *Journal of the Royal Statistical Society: Series A*, 164, 61-72.
- Kulldorff, M. (2007). *SaTScan user guide for version 7.0.3*. Retrieved from <http://www.satscan.org/techdoc.html>.
- Kulldorff, M., Athas, W. F., Feurer, E. J., Miller, B. A., & Key, C. A. (1998). Evaluating cluster alarms: a space-time scan statistic and brain cancer in Los Alamos, New Mexico. *American Journal of Public Health*, 88, 1377-1380.
- Kulldorff, M., & Information Management Services Inc. (2007). SaTScan: Software for the spatial and space-time scan statistics. Bethesda: National Cancer Institute.
- Salt Lake Valley Health Department - Bureau of Epidemiology (2008). *2007 cryptosporidiosis outbreak report*. Salt Lake Valley Health Department.

- U.S. Census Bureau (2000a). *Census 2000 block group cartographic boundary files – Utah*. U.S. Department of Commerce Economics and Statistics Administration. Retrieved from <http://www.census.gov/geo/www/cob/bg2000.html>.
- U.S. Census Bureau (2000b). *Summary File 1, P1 Total Population*. U.S. Department of Commerce Economics and Statistics Administration. Retrieved from <http://factfinder.census.gov/>.
- U.S. Census Bureau (2006). *2006 Population Estimates*. U.S. Department of Commerce Economics and Statistics Administration. Retrieved from <http://factfinder.census.gov/>.
- U.S. Census Bureau (2007). *2007 Population Estimates*. U.S. Department of Commerce Economics and Statistics Administration. Retrieved from <http://factfinder.census.gov/>.
- Utah Department of Health - Bureau of Epidemiology (2008). *Report of investigation: Cryptosporidium outbreak linked to multiple recreational water venues - Utah, 2007*. Utah Department of Health.
- Yoder, J. S., & Beach, M. J. (2007). Cryptosporidiosis surveillance - United States, 2003-2005. *MMWR Surveillance Summaries*, 56(SS-7), 1-10.
- Yoder, J. S., Hlavsa, M. C., Craun, G. F., Hill, V., Roberts, V., Yu, P. A., et al. (2008). Surveillance for waterborne disease and outbreaks associated with recreational water use and other aquatic facility-associated health events - United States, 2005-2006. *MMWR Surveillance Summaries*, 57(SS-9), 1-32.

Table 1. Space-time clusters from August 8 to September 11, 2007 (MMWR Weeks 32 - 37)

Clusters	Signal ID	Signal Date	Number of Days in Signal	Number of Block Groups in Cluster	Total Number of Cases in Time Step	Observed Cases in the Cluster	Expected Cases	Relative Risk	<i>p</i>	Recurrence Interval
Most Likely Cluster	1	8/8/07	2	1	20	3	0.01	581.767	0.001	Every 76.6 years
Most Likely Cluster	6	8/17/07	4	48	51	8	0.65	14.439	0.019	Every 3.99 years
Most Likely Cluster	8	8/21/07	2	14	76	6	0.20	32.821	0.006	Every 12.7 years
Secondary Cluster	8a	8/21/07	7	53	76	12	1.81	7.706	0.024	Every 3.1 years
Most Likely Cluster	11	8/24/07	5	14	127	11	0.83	14.467	0.001	Every 76.6 years
Secondary Cluster	11a	8/24/07	1	32	127	6	0.29	22.005	0.048	Every 1.5 years
Tertiary Cluster	11b	8/24/07	2	54	127	8	0.69	12.357	0.053	Every 1.4 years
Most Likely Cluster	21	9/7/07	4	23	342	25	2.81	9.507	0.001	Every 76.6 years
Secondary Cluster	21a	9/7/07	4	16	342	19	1.97	10.164	0.001	Every 76.6 years
Tertiary Cluster	21b	9/7/07	4	25	342	15	1.58	9.875	0.001	Every 76.6 years
Quaternary Cluster	21c	9/7/07	4	16	342	13	1.85	7.282	0.011	Every 6.9 years
Most Likely Cluster	25	9/11/07	7	23	401	25	5.77	4.552	0.001	Every 76.6 years
Secondary Cluster	25a	9/11/07	7	6	401	15	2.17	7.141	0.003	Every 25.5 years
Tertiary Cluster	25b	9/11/07	7	12	401	15	2.58	5.996	0.021	Every 3.6 years

List of Figures

Figure 1. Temporal length and general geographic regions of all significant space-time clusters detected from August 8 to September 11, 2007 (MMWR Weeks 32 - 37). Only signals with a recurrence interval of approximately 1 year are summarized in the graph.

Figure 2. Significant space-time clusters detected during six 28-day time steps from August 8 to September 11, 2007 (MMWR Weeks 32 - 37). Detailed information on the number of days in the signal, observed number of cases, expected number of cases, relative risk, p -value, and recurrence intervals for all clusters illustrated in these maps are presented in Table 1. The scale and orientation of all maps are the same as 2a.

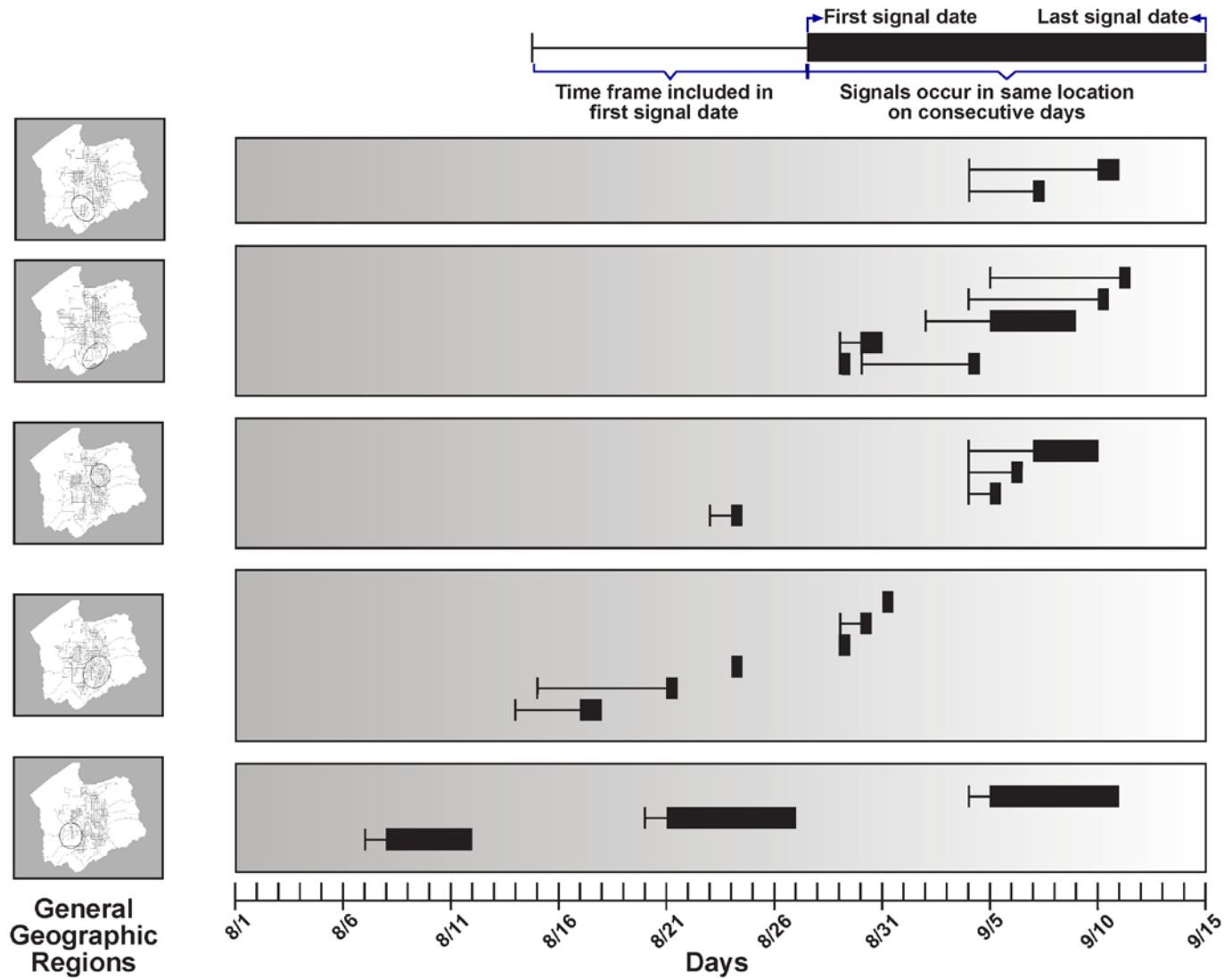


Figure 1.

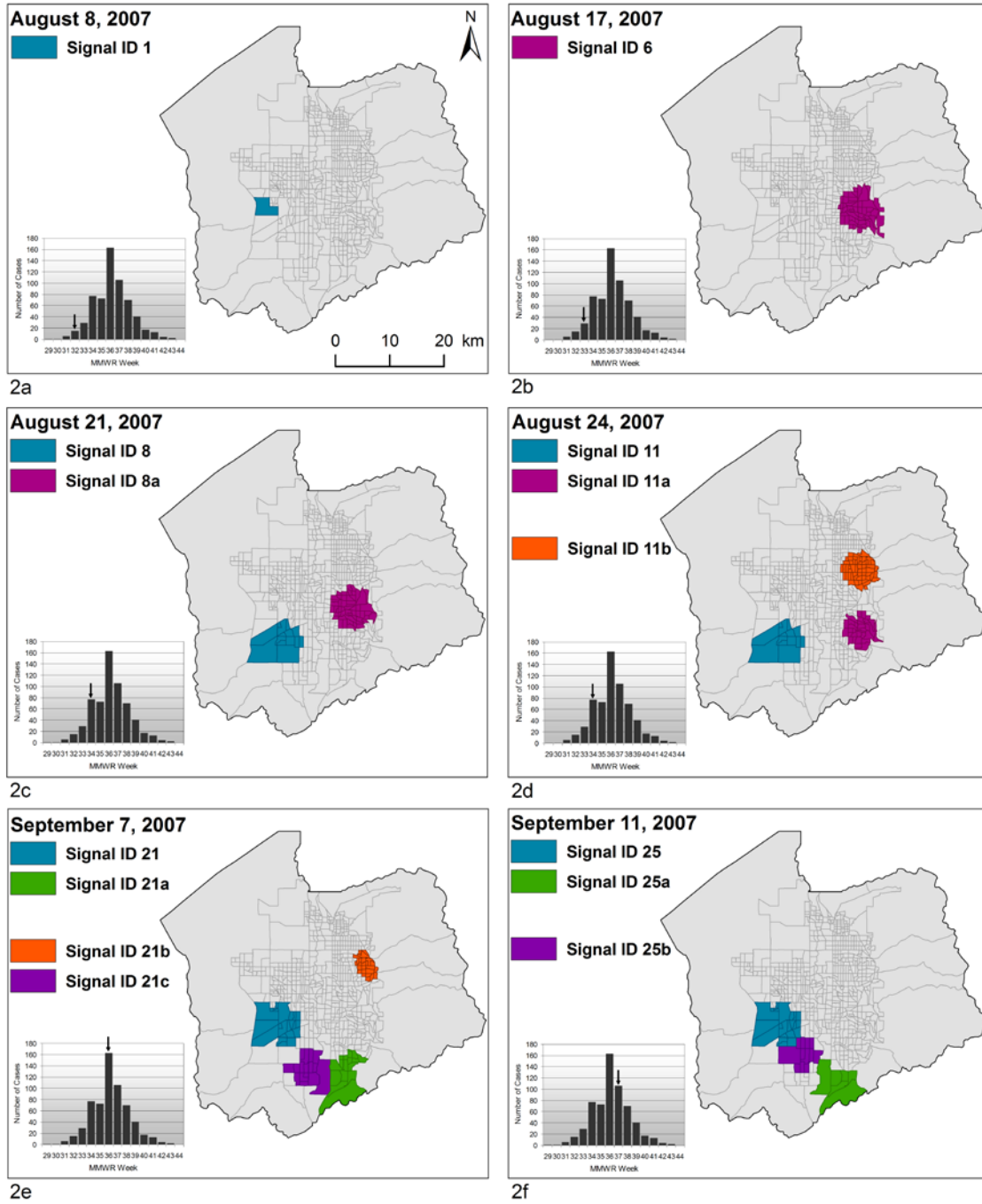


Figure 2